



Published in final edited form as:

*J Nucl Med.* 2008 May ; 49(5): 823–829. doi:10.2967/jnumed.107.048553.

## Lead-203-Labeled Alpha-Melanocyte Stimulating Hormone Peptide as an Imaging Probe for Melanoma Detection

Yubin Miao<sup>1,2,3</sup>, Said D. Figueroa<sup>4</sup>, Darrell R. Fisher<sup>5</sup>, Herbert A. Moore<sup>6</sup>, Richard F. Testa<sup>6</sup>, Timothy J. Hoffman<sup>4,7,8</sup>, and Thomas P. Quinn<sup>4,9,10</sup>

<sup>1</sup>College of Pharmacy, University of New Mexico, Albuquerque, NM 87131

<sup>2</sup>Cancer Research and Treatment Center, University of New Mexico, Albuquerque, NM 87131

<sup>3</sup>Department of Dermatology, University of New Mexico, Albuquerque, NM 87131

<sup>4</sup>Department of Veterans Affairs Medical Center, Columbia, MO 65201

<sup>5</sup>Pacific Northwest National Laboratory, Richland, WA 99352

<sup>6</sup>AlphaMed Inc., Acton, MA 01720

<sup>7</sup>Department of Internal Medicine, University of Missouri, Columbia, MO 65211, USA

<sup>8</sup>Department of Chemistry, University of Missouri, Columbia, MO 65211, USA

<sup>9</sup>Department of Biochemistry, University of Missouri, Columbia, MO 65211, USA

<sup>10</sup>Department of Radiology, University of Missouri, Columbia, MO 65211, USA

### Abstract

Peptide-targeted alpha therapy with 7.4 MBq of <sup>212</sup>Pb-[1,4,7,10-tetraazacyclododecane-1,4,7,10-tetraacetic acid-ReO-[Cys<sup>3,4,10</sup>, D-Phe<sup>7</sup>, Arg<sup>11</sup>] $\alpha$ -MSH<sub>3-13</sub> {<sup>212</sup>Pb-DOTA-Re(Arg<sup>11</sup>)CCMSH} cured 45% of B16/F1 murine melanoma-bearing C57 mice in a 120-day study, highlighting its melanoma treatment potential. However, there is a need to develop an imaging surrogate for patient-specific dosimetry and to monitor the tumor response to <sup>212</sup>Pb-DOTA-Re(Arg<sup>11</sup>)CCMSH therapy. The purpose of this study was to evaluate the potential of <sup>203</sup>Pb-DOTA-Re(Arg<sup>11</sup>)CCMSH as a matched-pair SPECT imaging agent for <sup>212</sup>Pb-DOTA-Re(Arg<sup>11</sup>)CCMSH.

**Method**—DOTA-Re(Arg<sup>11</sup>)CCMSH was labeled with <sup>203</sup>Pb in 0.5 M NH<sub>4</sub>OAc buffer at pH 5.4. The internalization and efflux of <sup>203</sup>Pb-DOTA-Re(Arg<sup>11</sup>)CCMSH were determined in B16/F1 melanoma cells. The pharmacokinetics of <sup>203</sup>Pb-DOTA-Re(Arg<sup>11</sup>)CCMSH was examined in B16/F1 melanoma-bearing C57 mice. A micro-SPECT/CT imaging study was performed with <sup>203</sup>Pb-DOTA-Re(Arg<sup>11</sup>)CCMSH in a B16/F1 melanoma-bearing C57 mouse at 2 h post-injection.

**Results**—Lead-203-DOTA-Re(Arg<sup>11</sup>)CCMSH was easily prepared in NH<sub>4</sub>OAc buffer and completely separated from the excess non-radiolabeled peptide by RP-HPLC. Lead-203-DOTA-Re(Arg<sup>11</sup>)CCMSH displayed fast internalization and extended retention in B16/F1 cells. Approximately 73% of <sup>203</sup>Pb-DOTA-Re(Arg<sup>11</sup>)CCMSH activity internalized after a 20-min incubation at 25°C. After incubating the cells in culture media for 20 min, 78% of internalized activity remained in the cells. Lead-203-DOTA-Re(Arg<sup>11</sup>)CCMSH exhibited similar biodistribution pattern with <sup>212</sup>Pb-DOTA-Re(Arg<sup>11</sup>)CCMSH in B16/F1 melanoma-bearing mice. Lead-203-DOTA-Re(Arg<sup>11</sup>)CCMSH exhibited the peak tumor uptake of 12.00±3.20 %ID/g at 1 h

**Corresponding Authors:** Thomas P. Quinn, 117 Schweitzer Hall, Department of Biochemistry, University of Missouri-Columbia, Columbia, MO 65211. Phone: (573) 882-6099; Fax: (573) 884-4812; quinnt@missouri.edu; Yubin Miao, 2502 Marble NE, MSC09 5360, College of Pharmacy, University of New Mexico, Albuquerque, NM 87113. Phone: (505) 925-4437; Fax: (505) 272-6749; ymiao@salud.unm.edu.

post-injection. The tumor uptake gradually decreased to  $3.43 \pm 1.12$  %ID/g at 48 h post-injection. Lead-203-DOTA-Re(Arg<sup>11</sup>)CCMSH exhibited a peak tumor to kidney uptake ratio of 1.53 at 2 h post-injection. The absorbed doses to the tumor and kidneys were 4.32 and 4.35 Gy/37 MBq, respectively. Whole-body clearance of <sup>203</sup>Pb-DOTA-Re(Arg<sup>11</sup>)CCMSH was fast, with approximately 89% of the injected activity cleared through urinary system by 2 h post-injection. Lead-203 showed 1.6 mm SPECT imaging resolution, which was comparable to <sup>99m</sup>Tc. Melanoma lesions were visualized through SPECT/CT images of <sup>203</sup>Pb-DOTA-Re(Arg<sup>11</sup>)CCMSH at 2 h post-injection.

**Conclusions**—Lead-203-DOTA-Re(Arg<sup>11</sup>)CCMSH exhibited favorable pharmacokinetic and tumor imaging properties, highlighting its potential as a matched-pair SPECT imaging agent for <sup>212</sup>Pb-DOTA-Re(Arg<sup>11</sup>)CCMSH melanoma treatment.

## Introduction

Investigators can predict the usefulness of new imaging and therapy agents based on the results of matched-pairs of identical or near identical radiopharmaceuticals. The advantage of taking a matched-pair approach is that the imaging agent can be used to demonstrate selective tumor targeting and to obtain patient-specific dosimetry, allowing optimal and safe deployment of the therapeutic counterpart. Some examples of matched-pair approaches have been the use of <sup>111</sup>In- and <sup>90</sup>Y-radiolabeled compounds such as octreotide (1-4) as well as <sup>99m</sup>Tc- and <sup>188</sup>Re-radiolabeled alpha-melanocyte stimulating hormone ( $\alpha$ -MSH) peptides (5-7). However, in the above cases, similar but not chemically identical radiometals were used. Even though the radiometals may have similar coordination chemistries, small differences among radionuclides can result in different pharmacokinetics (8, 9). Therefore, it is desirable to radiolabel the targeting compound with two chemically identical radioisotopes to extract the maximum benefit from the matched-pair approach to radiopharmaceutical design.

Peptide-targeted alpha-particle therapy for melanoma using <sup>212</sup>Pb-radiolabeled DOTA-Re(Arg<sup>11</sup>)CCMSH was reported in our previous publication (10). The results demonstrated that the peptide-targeted alpha-particle therapy was effective in increasing the mean survival times of mice initially bearing melanoma tumors. Treatment with single doses of 3.7 or 7.4 MBq of <sup>212</sup>Pb-DOTA-Re(Arg<sup>11</sup>)CCMSH resulted in 20% and 45% of animals with complete cures, respectively. The development of a matched-pair imaging agent counterpart for <sup>212</sup>Pb-DOTA-Re(Arg<sup>11</sup>)CCMSH would be very useful to demonstrate tumor uptake and for calculating the dose to normal tissues and vital organs. Patient-specific dosimetry determined from the imaging studies would be useful for treatment planning so that the maximum tolerable activity of the alpha-particle emitting radiolabeled peptide could be administered for safe and effective melanoma treatment. Moreover, a matched-pair imaging agent could be utilized to further monitor the patients' response to the targeted alpha-radiation therapy.

A potential matched-pair imaging radioisotope for the therapeutic radionuclide <sup>212</sup>Pb is <sup>203</sup>Pb (11-14). Upon decay, <sup>203</sup>Pb ( $T_{1/2}$ =51.9 h) emits a 279 keV gamma ray (81% abundance) suitable for SPECT imaging. Lead-203 can be produced via the <sup>203</sup>Tl(d, 2n)<sup>203</sup>Pb reaction by irradiating natural Tl<sub>2</sub>O<sub>3</sub> or enriched Tl<sub>2</sub>O<sub>3</sub>(<sup>203</sup>Tl) target with 13.7 MeV deuterons (11). A simple and rapid procedure was reported for purifying cyclotron-produced <sup>203</sup>Pb via the <sup>203</sup>Tl(d,2n)<sup>203</sup>Pb reaction (11). High specific activity and radiochemical purity of <sup>203</sup>Pb are essential for radiolabeling peptides that target lower copy number cellular receptors. Low radiochemical purity of <sup>203</sup>Pb can dramatically reduce if not eliminate the radiolabeling yields due to the competition of the existing contaminating metals. Likewise, low specific activity of <sup>203</sup>Pb preparations may result in the saturation of

the targeted receptors with non-radioactively labeled peptides. Purified  $^{203}\text{Pb}$  was used to label the monoclonal antibody Herceptin, which was shown to be immunoreactive and displayed favorable biodistribution properties *in vivo*, demonstrating the suitability and feasibility of  $^{203}\text{Pb}$  labeled biomolecules to target cellular antigens (11).

In this study, DOTA-Re(Arg<sup>11</sup>)CCMSH (5, 8) was radiolabeled with  $^{203}\text{Pb}$  to evaluate its potential as a matched-pair imaging agent for  $^{212}\text{Pb}$ -DOTA-Re(Arg<sup>11</sup>)CCMSH. The spatial resolution of  $^{203}\text{Pb}$  was examined through a hot-rod phantom imaging by small animal SPECT and compared with that of  $^{99\text{m}}\text{Tc}$ . The melanocortin-1 (MC1) receptor-mediated uptake and efflux of  $^{203}\text{Pb}$ -DOTA-Re(Arg<sup>11</sup>)CCMSH were examined *in vitro*. Biodistribution and SPECT imaging studies were performed to demonstrate the potential of  $^{203}\text{Pb}$ -DOTA-Re(Arg<sup>11</sup>)CCMSH to image the melanoma lesions.

## Materials and Methods

### Chemicals and Reagents

DOTA-Re(Arg<sup>11</sup>)CCMSH was purchased from Bachem Inc. (King of Prussian, PA). Lead-203 was obtained from AlphaMed, Inc (Acton, MA). All other chemicals used in this study were purchased from Fischer Scientific (Waltham, MA) and used without further purification. The B16/F1 murine melanoma cell line was obtained from American Type Culture Collection (Manassas, VA).

### Calibration of SPECT detector with $^{203}\text{Pb}$

A high count flood image was acquired with 0.37 MBq of  $^{203}\text{Pb}$ , placed in the central axis above the detector face, employing uncollimated detectors. Energy discriminating windows were employed for photopeak isolation of the  $^{203}\text{Pb}$  spectrum. Detector non-uniformities arise due to the detector crystal-to-crystal detection efficiency variability and pinhole sensitivity changes associated with the angle of acceptance of the pinhole aperture. To correct the detector non-uniformity, all projection images were normalized to  $^{203}\text{Pb}$  with a correction matrix derived from the collected  $^{203}\text{Pb}$  uniform flood image.

### Jaszczak SPECT Phantom Imaging

SPECT volumetric performance for  $^{203}\text{Pb}$  was assessed using a micro-Deluxe ECT hot insert phantom (Data Spectrum Inc., NC). The phantom had an inner diameter of 4.4 cm with six equally-sized rod quadrants. The rod diameters were 1.2, 1.6, 2.4, 3.2, 4.0 and 4.8 mm, respectively. The phantom was filled with 74 MBq of  $^{203}\text{Pb}$  and was imaged with a 1.0 mm pinhole and a magnification factor of 2 at a distance of 4.5 cm. The SPECT scan was acquired for 60 frames over 360 degrees and the projection data were reconstructed using a 3D-OSEM algorithm. The phantom SPECT data were reconstructed using 12 iterations and 4 subsets. The reconstructed images were smoothed post reconstruction with a 3D Gaussian kernel. A parallel study was performed with  $^{99\text{m}}\text{Tc}$  for comparison.

### Synthesis of $^{203}\text{Pb}$ -DOTA-Re(Arg<sup>11</sup>)CCMSH

DOTA-Re(Arg<sup>11</sup>)CCMSH was radiolabeled with  $^{203}\text{Pb}$  in 0.5 M  $\text{NH}_4\text{OAc}$  at pH 5.4. Briefly, 50  $\mu\text{l}$  of  $^{203}\text{PbCl}_2$  in 0.5 M HCl (~37 MBq), 500  $\mu\text{L}$  of 0.5 M  $\text{NH}_4\text{OAc}$  (pH 5.4) and 20  $\mu\text{L}$  of 1 mg/mL DOTA-Re(Arg<sup>11</sup>)CCMSH were added into a reaction vial and incubated at 75°C for 40 min. Lead-203-DOTA-Re(Arg<sup>11</sup>)CCMSH was purified to single species by Waters HPLC (Franklin, MA) on a Vydac C-18 reverse phase analytical column (Deerfield, IL) using a 20-min linear gradient of 16-26% acetonitrile in 20 mM HCl aqueous solution with a flowrate of 1.5 ml/min. The stability of  $^{203}\text{Pb}$ -DOTA-Re(Arg<sup>11</sup>)CCMSH was monitored up to 24 h for degradation by HPLC in 0.1% BSA in 10 mM phosphate-buffered saline (PBS) at 37°C. HPLC purified peptide samples were purged with  $\text{N}_2$  gas for

20 min to remove the acetonitrile. The pH of final solution was adjusted to 5 with 0.1 N NaOH and diluted with normal saline for animal studies.

### Cellular Internalization and Efflux of $^{203}\text{Pb}$ -DOTA-Re(Arg<sup>11</sup>)CCMSH

B16/F1 murine melanoma cells were obtained from American Type Culture Collection and cultured in RPMI 1640 media containing  $\text{NaHCO}_3$  (2 g/l), supplemented with 10% heat-inactivated fetal calf albumin (FCA), 2 mM *L*-glutamine, and 48 mg of gentamicin. The cells were incubated at 37°C in 75 cm<sup>3</sup> tissue culture flasks under a humidified 5% CO<sub>2</sub> atmosphere. The culture media were changed every two days. Cellular internalization and efflux of  $^{203}\text{Pb}$ -DOTA-Re(Arg<sup>11</sup>)CCMSH were evaluated in B16/F1 murine melanoma cells. B16/F1 cells ( $5 \times 10^5$ /well) were seeded into a 24-well cell culture plate and incubated at 37°C overnight. After being washed once with binding media (MEM with 25 mM HEPES, pH 7.4, 0.2% BSA, 0.3 mM 1,10-phenanthroline), the cells were incubated at 25°C for 20, 40, 60, 90 and 120 min (n=4) in the presence of approximately 100,000 counts per minute (cpm) of HPLC purified  $^{203}\text{Pb}$ -DOTA-Re(Arg<sup>11</sup>)CCMSH. After incubation, the reaction medium was aspirated and cells were rinsed with 2×0.5 mL of ice-cold pH 7.4, 0.2% BSA / 0.01 M PBS. Cellular internalization of  $^{203}\text{Pb}$ -DOTA-Re(Arg<sup>11</sup>)CCMSH was assessed by washing the cells with acidic buffer [40 mM sodium acetate (pH 4.5) containing 0.9% NaCl and 0.2% BSA] to remove the membrane bound radioactivity. The remaining internalized radioactivity was obtained by lysing the cells with 0.5 mL of 1N NaOH for 5 min. Membrane-bound and internalized  $^{203}\text{Pb}$  activity was counted in a gamma counter. Cellular efflux of  $^{203}\text{Pb}$ -DOTA-Re(Arg<sup>11</sup>)CCMSH was determined by incubating B16/F1 cells with  $^{203}\text{Pb}$ -DOTA-Re(Arg<sup>11</sup>)CCMSH for 2 h at 25°C, removing non-specific bound activity with 2×0.5 mL of ice-cold pH 7.4, 0.2% BSA / 0.01 M PBS rinse, and monitoring radioactivity released into cell culture media. The radioactivity in media, on cell surface and in cells were separately collected and counted in a gamma counter 20, 40, 60, 90 and 120 min post incubation in the culture media.

### Biodistribution studies

Animal studies were conducted in compliance with Institutional Animal Care and Use Committee approval. Pharmacokinetic studies were performed in C57 mice that were inoculated subcutaneously with  $1 \times 10^6$  B16/F1 murine melanoma cells in the right flank. When the weight of tumors reached approximately 0.2 g,  $7.4 \times 10^{-3}$  MBq of  $^{203}\text{Pb}$ -DOTA-Re(Arg<sup>11</sup>)CCMSH was injected into each mouse through the tail vein. Groups of 5 mice per each time point were used for the biodistribution studies. The mice were sacrificed at 5 min, 30 min, 1, 2, 4, 24 and 48 h post-injection, and tumors and organs of interest (whole organs except muscle, bone and skin) were harvested, weighed and counted in a Wallac 1480 automated gamma counter. The results were expressed as percent injected dose/gram (%ID/g) and as percent injected dose (%ID). Blood values were taken as 6.5% of the whole body weight. Partial parts of muscle, bone and skin were collected and weighed for calculating %ID/g in those organs. The tumor uptake specificity of  $^{203}\text{Pb}$ -DOTA-Re(Arg<sup>11</sup>)CCMSH was determined by blocking tumor uptake at 2 h post-injection with the co-injection of 10 μg of unlabeled [Nle<sup>4</sup>, D-Phe<sup>7</sup>]α-MSH (NDP-MSH), a linear α-MSH peptide analog with picomolar affinity for the α-MSH receptor present on murine melanoma cells.

### Dosimetry Calculation

The biodistribution of  $^{203}\text{Pb}$ -DOTA-Re(Arg<sup>11</sup>)CCMSH over time was determined to evaluate uptake and retention, and to calculate radiation absorbed doses from  $^{203}\text{Pb}$ -DOTA-Re(Arg<sup>11</sup>)CCMSH in tumors, normal organs and tissues using methods described previously (15-17). Time-activity curves were generated for 16 organs and tissues (blood, bone, brain, heart, lung, liver, skin, spleen, stomach, kidney, large intestine, small intestine, muscle, pancreas, carcass and tumor). Cumulative activity of  $^{203}\text{Pb}$  was determined for each organ

by integrating the area under the time-activity curves. The cumulative activity were then used with a dosimetric model (15, 16) developed specifically for the laboratory mouse.

### Melanoma Imaging with $^{203}\text{Pb}$ -DOTA-Re(Arg $^{11}$ )CCMSH

One B16/F1 melanoma-bearing C57 mouse was injected with 6.29 MBq of HPLC-purified  $^{203}\text{Pb}$ -DOTA-Re(Arg $^{11}$ )CCMSH via the tail vein 14 days after cell implantation. The mouse was euthanized by CO $_2$  inhalation for Micro-CT/SPECT imaging at 2 h post-injection. The SPECT data were collected right after CT data collection. Approximately 0.3 MBq of  $^{203}\text{Pb}$ -DOTA-Re(Arg $^{11}$ )CCMSH activity left in the mouse at the moment of acquisition. Micro-SPECT scans of 60 frames for the animal were acquired for a total count acquisition of 0.5 million counts for  $^{203}\text{Pb}$ -DOTA-Re(Arg $^{11}$ )CCMSH. A pinhole magnification factor of 2.2 was used in the experiments. The micro-SPECT/CT images were obtained using the MicroCAT II $^{\text{TM}}$  CT/SPECT from Siemens Pre-Clinical Solutions (Knoxville, TN) equipped with high resolution SPECT pinhole collimators. The SPECT projection data (78 $\times$ 78 $\times$ 102 matrix) were reconstructed employing a 3D-OSEM algorithm with geometrical misalignment corrections and the CT raw data were reconstructed via a cone beam (Feldkamp) filtered back projection algorithm. Reconstructed data from SPECT and CT were visualized and co-registered using Amira 3.1 (TGS, San Diego, CA).

## Results

Tomographic spatial resolution of 1.6 mm was achieved with the micro-Deluxe ECT hot-rod  $^{203}\text{Pb}$  SPECT phantom at a distance of 4.5 cm (Fig. 1). Comparing the transaxial slice of the  $^{203}\text{Pb}$  reconstructed volumetric SPECT data with the same phantom filled with 74 MBq of  $^{99\text{m}}\text{Tc}$ , The results were comparable when considering the 4.8-1.6 mm quadrant regions and the differentiation of rods within the phantom quadrants.

DOTA-Re(Arg $^{11}$ )CCMSH was labeled with  $^{203}\text{Pb}$  using a 0.5 M NH $_4$ OAc-buffered solution at pH 5.4. Lead-203-DOTA-Re(Arg $^{11}$ )CCMSH was completely separated from its non-radiolabeled counterpart by RP-HPLC. The stability of  $^{203}\text{Pb}$ -DOTA-Re(Arg $^{11}$ )CCMSH was determined by incubation in 0.1% BSA in 10 mM PBS (pH 7.4) at 37 $^{\circ}\text{C}$ . Only the  $^{203}\text{Pb}$ -labeled peptide was detected by RP-HPLC after 24 h incubation. A schematic structure of  $^{203}\text{Pb}$ -DOTA-Re(Arg $^{11}$ )CCMSH is presented in Fig. 2. Cellular internalization and efflux of  $^{203}\text{Pb}$ -DOTA-Re(Arg $^{11}$ )CCMSH were evaluated in B16/F1 cells at 25 $^{\circ}\text{C}$ . Figure 3 illustrates the cellular internalization and efflux of  $^{203}\text{Pb}$ -DOTA-Re(Arg $^{11}$ )CCMSH. Lead-203-DOTA-Re(Arg $^{11}$ )CCMSH exhibited rapid cellular internalization. Approximately 73% and 74% of  $^{203}\text{Pb}$ -DOTA-Re(Arg $^{11}$ )CCMSH activity were internalized in the B16/F1 cells after 20 min and 2 h incubation, respectively. Cellular efflux of  $^{203}\text{Pb}$ -DOTA-Re(Arg $^{11}$ )CCMSH demonstrated that 78% and 40% of the  $^{203}\text{Pb}$  activity remained inside the cells 20 min and 2 h after incubating cells in culture medium at 25 $^{\circ}\text{C}$ , respectively.

The pharmacokinetics and tumor targeting properties of  $^{203}\text{Pb}$ -DOTA-Re(Arg $^{11}$ )CCMSH were determined in B16/F1 murine melanoma-bearing C57 mice. The biodistribution of  $^{203}\text{Pb}$ -DOTA-Re(Arg $^{11}$ )CCMSH is shown in Table 1. Lead-203-DOTA-Re(Arg $^{11}$ )CCMSH exhibited high uptake and long retention in the tumor. At 1 h post-injection,  $^{203}\text{Pb}$ -DOTA-Re(Arg $^{11}$ )CCMSH reached its peak tumor uptake value of  $12.00\pm 3.20$  %ID/g. There was  $9.86\pm 1.86$  %ID/g of  $^{203}\text{Pb}$ -DOTA-Re(Arg $^{11}$ )CCMSH activity remained in the tumor at 4 h post-injection. The tumor uptake value gradually decreased to  $4.35\pm 0.24$  %ID/g at 24 h and  $3.43\pm 1.12$  %ID/g at 48 h post-injection. Tumor uptake specificity of  $^{203}\text{Pb}$ -DOTA-Re(Arg $^{11}$ )CCMSH was examined by co-injecting 10  $\mu\text{g}$  of the high affinity  $\alpha$ -MSH peptide analogue NDP-MSH. The tumor uptake of  $^{203}\text{Pb}$ -DOTA-Re(Arg $^{11}$ )CCMSH with NDP co-injection was only 7.3% of the tumor uptake

without NDP co-injection at 2 h after dose administration ( $P < 0.01$ ), demonstrating that tumor uptake was specific and receptor-mediated. Whole-body clearance of  $^{203}\text{Pb}$ -DOTA-Re(Arg<sup>11</sup>)CCMSH was very rapid, with approximately 90% of the injected dose was washed out of the body by 2 h post-injection. Ninety-four percent of the injected dose was washed out of the body by 24 h post-injection. Normal organ uptakes of  $^{203}\text{Pb}$ -DOTA-Re(Arg<sup>11</sup>)CCMSH were generally very low ( $< 1\%$  ID/g) at 2 h post-injection except for the kidneys. High tumor/blood and tumor/normal organ uptake ratios were demonstrated as early as 30 min post-injection (Table 1). The kidneys appeared to be the major excretion organ of  $^{203}\text{Pb}$ -DOTA-Re(Arg<sup>11</sup>)CCMSH. The kidney uptake values of  $^{203}\text{Pb}$ -DOTA-Re(Arg<sup>11</sup>)CCMSH were  $7.78 \pm 1.42\%$  ID/g and  $3.69 \pm 0.58\%$  ID/g at 2 and 24 h post-injection, respectively. Bone uptake values of  $^{203}\text{Pb}$ -DOTA-Re(Arg<sup>11</sup>)CCMSH activity were less than  $1.4\%$  ID/g at all time points after 1 h post-injection in this study.

The absorbed radiation doses to tumors and normal organs from  $^{203}\text{Pb}$ -DOTA-Re(Arg<sup>11</sup>)CCMSH were determined in this study from the biodistribution data in B16/F1 murine melanoma-bearing mice (Table 2). The absorbed dose from  $^{203}\text{Pb}$ -DOTA-Re(Arg<sup>11</sup>)CCMSH in the B16/F1 mouse tumors was  $4.32\text{ Gy}/37\text{ MBq}$ . The relatively high tumor dose was directly related to the rapid uptake kinetics and retention of the  $^{203}\text{Pb}$ -labeled peptide. Normal tissue doses were low except for the kidneys, which were estimated at  $4.35\text{ Gy}/37\text{ MBq}$ . These results suggest that the kidneys may be the dose-limiting normal organ for radionuclide therapy. One B16/F1 murine melanoma-bearing C57 mouse was injected with  $^{203}\text{Pb}$ -DOTA-Re(Arg<sup>11</sup>)CCMSH to visualize the tumor at 2 h after dose administration (Fig. 4). Although there was substantial activity in the kidneys, melanoma tumors in the right flank were visualized clearly at 2 h post-injection. Lead-203-DOTA-Re(Arg<sup>11</sup>)CCMSH exhibited high tumor to normal organ uptake ratios except for the kidney in the SPECT image, which was coincident with the trend observed in the biodistribution of  $^{203}\text{Pb}$ -DOTA-Re(Arg<sup>11</sup>)CCMSH.

## Discussion

Radiolabeled  $\alpha$ -MSH peptide analogues as imaging agents may have their greatest utility when used in a matched-pair approach for melanoma radionuclide therapy. In a matched-pair approach to radionuclide therapy, the same melanoma targeting peptide can be labeled with radioisotopes possessing diagnostic imaging or therapeutic decay properties. The advantage of this approach is that patient-specific dosimetry can be determined using the imaging agent so that the optimal dose of the peptide labeled with the therapeutic radioisotope can be administered. Moreover, a matched-pair imaging agent could be utilized to further monitor the patients' response to the targeted radionuclide therapy.  $^{111}\text{In}$ -labeled conjugates are often used as imaging surrogates for dosimetric calculation of  $^{90}\text{Y}$ -labeled conjugates based on the assumption that  $^{90}\text{Y}$ - and  $^{111}\text{In}$ -labeled conjugates are chemically and biologically equivalent. However,  $^{90}\text{Y}$ - and  $^{111}\text{In}$ -labeled monoclonal antibody and peptide showed differences in their biological properties (8, 9, 18), which raised some concerns on the validity of using  $^{111}\text{In}$ -labeled conjugates as imaging surrogates for their  $^{90}\text{Y}$ -labeled conjugates. The atomic radius of  $^{90}\text{Y}$  fits nearly perfectly into the cavity of DOTA, whereas  $^{111}\text{In}$  has a smaller atomic radius than that of  $^{90}\text{Y}$ . The biodistribution differences between  $^{111}\text{In}$ - and  $^{90}\text{Y}$ -labeled conjugates are likely to be related to the different coordination chemistries in solution (9, 19, 20). Hence, radiolabeling the targeting compound with two radioisotopes of the same metal will maximally extract the benefit from the matched-pair approach to radiopharmaceutical development for cancer imaging and therapy.

Lead-212-DOTA-Re(Arg<sup>11</sup>)CCMSH was used for targeted alpha-radiation therapy for melanoma in our previous studies (10). DOTA-Re(Arg<sup>11</sup>)CCMSH exhibited nanomolar

MC1 receptor binding affinity and specifically targeted  $^{212}\text{Pb}$  to melanoma cells. Lead-212 decays via beta-emission to  $^{212}\text{Bi}$  which subsequently decays via a branched pathway to stable  $^{208}\text{Pb}$ , yielding high-energy  $\alpha$ -particles and  $\beta$ -particles (10). High cytotoxic ionizing radiation from alpha-particles results in irreparable DNA double strand breaks, causing cell death. A major advantage of administering  $^{212}\text{Pb}$ -DOTA-Re(Arg<sup>11</sup>)CCMSH is that the radiolabeled peptide will circulate, target melanoma tumor cells and be cleared from the body as the  $^{212}\text{Pb}$ -labeled peptide rather than the alpha-emitting  $^{212}\text{Bi}$  compound, minimizing normal tissue exposures. Peptide-targeted  $^{212}\text{Pb}$  internalized and retained by tumor cells will decay to the alpha-particle emitting  $^{212}\text{Bi}$  and serve as an *in vivo* generator of alpha-particles, localizing the highly toxic short-ranged alpha-radiation within the tumor. Meanwhile, the 10.6 h half-life of  $^{212}\text{Pb}$  makes dose preparation and administration easier and more efficient than the short half-life ( $T_{1/2}$ =60.6 min)  $^{212}\text{Bi}$ . Lead-212-DOTA-Re(Arg<sup>11</sup>)CCMSH exhibited remarkable therapeutic efficacy in B16/F1 melanoma-bearing mice in our previous report (10). The treatment of 7.4 MBq of  $^{212}\text{Pb}$ -DOTA-Re(Arg<sup>11</sup>)CCMSH cured 45% of B16/F1 murine melanoma-bearing C57 mice in a 120-day study, highlighted its potential as a novel agent for targeted radionuclide therapy of melanoma.

Lead-203 and  $^{212}\text{Pb}$  are two isotopes with diagnostic and therapeutic properties (11, 12). The favorable decay and imaging properties of  $^{203}\text{Pb}$  make it an ideal matched-pair radioisotope for  $^{212}\text{Pb}$  for targeted radionuclide therapy (11, 12). Lead-203 is a manageable radioisotope with respect to dose preparation and waste disposal due to its half-life of 51.9 hours. Lead-203 displayed a comparable spatial resolution (1.6 mm) with  $^{99\text{m}}\text{Tc}$  (Fig. 1), demonstrating the suitability and feasibility of  $^{203}\text{Pb}$  as a SPECT imaging isotope. Moreover,  $^{203}\text{Pb}$  can be produced via the  $^{203}\text{Tl}(d,2n)^{203}\text{Pb}$  reaction by a cyclotron and can be easily purified to achieve high specific activity for radiolabeling of antibodies or peptides for antigen or receptor targeting (11). In this study,  $^{203}\text{Pb}$ -DOTA-Re(Arg<sup>11</sup>)CCMSH was prepared and evaluated *in vitro* and in melanoma-bearing mice to evaluate its potential as a matched-pair imaging agent for  $^{212}\text{Pb}$ -DOTA-Re(Arg<sup>11</sup>)CCMSH.

*In vitro*,  $^{203}\text{Pb}$ -DOTA-Re(Arg<sup>11</sup>)CCMSH exhibited rapid cellular internalization and moderate retention. Tumor cell retention of  $^{203}\text{Pb}$ -DOTA-Re(Arg<sup>11</sup>)CCMSH at 40 min was approximately 50% compared to 87% and 90% for  $^{90}\text{Y}$ - and  $^{177}\text{Lu}$ -labeled DOTA-Re(Arg<sup>11</sup>)CCMSH, respectively (9). The greater efflux rate for  $^{203}\text{Pb}$ -DOTA-Re(Arg<sup>11</sup>)CCMSH was potentially due to the 2+ oxidation state of  $^{203}\text{Pb}$  coupled with the presence of the metal chelator phenanthroline in the cell binding and efflux media which lead to its accelerated release *in vitro*. However, *in vivo* higher tumor efflux kinetics for  $^{203}\text{Pb}$ -DOTA-Re(Arg<sup>11</sup>)CCMSH were not observed from 1 h to 4 h post-injection. The tumor uptake reached its peak value of  $12.00 \pm 3.20$  %ID/g at 1 h post-injection. *In vivo* tumor retention of  $^{203}\text{Pb}$ -DOTA-Re(Arg<sup>11</sup>)CCMSH remained constant at 2 h post injection (Table 2) leading to the high imaging contrast between the tumor and normal tissues. The tumor uptake value at 4 h post-injection was 81.2% of the tumor uptake value at 2 h post-injection (Table 2). Clearance of activity from the normal organs and tissues was rapid, which resulted in high tumor/blood and tumor/normal organ uptake ratios as early as 30 min post-injection (Table 1). The majority of the administered activity cleared through the kidneys, with approximately 89% of the injected dose being excreted in the urine by 2 h post injection. Co-injection of excess non-radioactive NDP-MSH peptide dramatically reduced tumor uptake but did not affect radioactivity in the kidneys, demonstrating that radioactivity in the tumor was receptor-mediated while the renal radioactivity was non-specific. The dosimetry results (Table 2) demonstrated that the absorbed dose to tumor and kidneys were approximately 8 times or greater than the absorbed dose to other normal organs, suggesting that the kidneys would be the dose-limiting normal organ for targeted radionuclide therapy. The statistical analyses of the tumor and kidney uptake values were performed

between  $^{203}\text{Pb}$ -DOTA-Re(Arg<sup>11</sup>)CCMSH and  $^{212}\text{Pb}$ -DOTA-Re(Arg<sup>11</sup>)CCMSH to confirm the matched-pair properties between  $^{203}\text{Pb}$  and  $^{212}\text{Pb}$  (data not shown). There were no significant difference ( $P>0.05$ ) in the tumor uptake values between  $^{203}\text{Pb}$ -DOTA-Re(Arg<sup>11</sup>)CCMSH and  $^{212}\text{Pb}$ -DOTA-Re(Arg<sup>11</sup>)CCMSH 1, 2, 4, 24 and 48 h post-injection. No significant differences ( $P>0.05$ ) exhibited in the kidney uptake values between  $^{203}\text{Pb}$ -DOTA-Re(Arg<sup>11</sup>)CCMSH and  $^{212}\text{Pb}$ -DOTA-Re(Arg<sup>11</sup>)CCMSH 1, 2 and 24 h post-injection. Overall, the in vivo biodistribution and clearance kinetics of  $^{203}\text{Pb}$ -DOTA-Re(Arg<sup>11</sup>)CCMSH were nearly identical to  $^{212}\text{Pb}$ -DOTA-Re(Arg<sup>11</sup>)CCMSH (10) in B16/F1 melanoma tumor bearing mice, confirming its matched-pair properties.

LS-174T colon carcinoma xenografts were successfully imaged by others with a  $^{203}\text{Pb}$ -DOTA-B72.3 antibody conjugate by a gamma camera at 120 h post-injection (12), highlighting the potential of radiolabeling the antibody with  $^{203}\text{Pb}$  to target the antigen for tumor imaging. In our study, dual-modality micro-SPECT/CT imaging was employed to evaluate the potential of  $^{203}\text{Pb}$ -DOTA-Re(Arg<sup>11</sup>)CCMSH as a melanoma imaging probe in a melanoma mouse model. Co-registration of high spatial resolution micro-CT anatomic data combined with molecular imaging data obtained using micro-SPECT allowed accurate identification and localization of the melanoma tumors. Flank melanoma tumors were clearly visualized with  $^{203}\text{Pb}$ -DOTA-Re(Arg<sup>11</sup>)CCMSH at 2 h post-injection by SPECT/CT images (Fig. 4). The SPECT imaging of tumors accurately matched the anatomical information from CT images. Lead-203-DOTA-Re(Arg<sup>11</sup>)CCMSH displayed high tumor to normal organ uptake ratios except for the kidneys in the SPECT/CT images, which was coincident with the trend observed in the biodistribution results (Table 1). High melanoma uptake and tumor to normal organ uptake ratios in SPECT/CT images validated the feasibility of  $^{203}\text{Pb}$ -DOTA-Re(Arg<sup>11</sup>)CCMSH as a matched-pair imaging agent for  $^{212}\text{Pb}$ -DOTA-Re(Arg<sup>11</sup>)CCMSH, which appears to be a promising peptide radiopharmaceutical for targeted radionuclide therapy of melanoma.

## Conclusions

Lead-203-DOTA-Re(Arg<sup>11</sup>)CCMSH exhibited high melanoma uptake and similar biodistribution pattern with  $^{212}\text{Pb}$ -DOTA-Re(Arg<sup>11</sup>)CCMSH, highlighting its potential as a matched-pair imaging probe for  $^{212}\text{Pb}$ -DOTA-Re(Arg<sup>11</sup>)CCMSH. In combination with SPECT/CT imaging equipment,  $^{203}\text{Pb}$ -DOTA-Re(Arg<sup>11</sup>)CCMSH could provide an effective approach to optimize the therapeutic doses using patient-specific dosimetry calculations and monitoring patient response to the targeted radionuclide therapy with  $^{212}\text{Pb}$ -DOTA-Re(Arg<sup>11</sup>)CCMSH.

## Acknowledgments

The authors express their gratitude to Drs. Wynn A. Volkert and Susan L. Deutscher for their helpful discussions and Ms. Katherine Benwell and Tiffani Shelton for their technical assistance. This work was supported by National Cancer Institute Grant 1R43 CA11492 and P50 Imaging Center Grant P50-CA-103130, the VA Biomolecular Imaging Center at the Harry S. Truman VA Hospital and the University of Missouri-Columbia, UNM-LANL MOU on Research and Education Grant 2R76T, American Foundation for Pharmaceutical Education Grant 3R48E and American Cancer Society Institutional Research Grant IRG-92-024.

### Financial Support:

This work was supported by National Cancer Institute Grant 1R43 CA11492 and P50 Imaging Center Grant P50-CA-103130, the VA Biomolecular Imaging Center at the Harry S. Truman VA Hospital and the University of Missouri-Columbia, UNM-LANL MOU on Research and Education Grant 2R76T, American Foundation for Pharmaceutical Education Grant 3R48E and American Cancer Society Institutional Research Grant IRG-92-024.

## References

1. De Jong M, Bakker WH, Krenning EP, Breeman WA, van der Pluijm ME, Bernard BF, Visser TJ, Jermann E, Behe M, Powell P, Macke HR. Yttrium-90 and indium-111 labelling, receptor binding and biodistribution of [DOTA<sup>0</sup>,d-Phe<sup>1</sup>,Tyr<sup>3</sup>]octreotide, a promising somatostatin analogue for radionuclide therapy. *Eur J Nucl Med*. 1997; 24:368–371. [PubMed: 9096086]
2. Forster GJ, Engelbach MJ, Brockmann JJ, Reber HJ, Buchholz HG, Macke HR, Rosch FR, Herzog HR, Bartenstein PR. Preliminary data on biodistribution and dosimetry for therapy planning of somatostatin receptor positive tumours: comparison of <sup>86</sup>Y-DOTATOC and <sup>111</sup>In-DTPA-octreotide. *Eur J Nucl Med*. 2001; 28:1743–1750. [PubMed: 11734910]
3. Helisch A, Forster GJ, Reber H, Buchholz HG, Arnold R, Goke B, Weber MM, Wiedenmann B, Pauwels S, Haus U, Bouterfa H, Bartenstein P. Pre-therapeutic dosimetry and biodistribution of <sup>86</sup>Y-DOTA-Phe1-Tyr3-octreotide versus <sup>111</sup>In-pentetreotide in patients with advanced neuroendocrine tumours. *Eur J Nucl Med Mol Imaging*. 2004; 31:1386–1392. [PubMed: 15175836]
4. Stahl A, Schachoff S, Beer A, Winter A, Wester HJ, Scheidhauer K, Schwaiger M, Wolf I. [<sup>111</sup>In]DOTATOC as a dosimetric substitute for kidney dosimetry during [<sup>90</sup>Y]DOTATOC therapy: results and evaluation of a combined gamma camera/probe approach. *Eur J Nucl Med Mol Imaging*. 2006; 33:1328–1336. [PubMed: 16645839]
5. Miao Y, Benwell K, Quinn TP. <sup>99m</sup>Tc and <sup>111</sup>In labeled alpha-melanocyte stimulating hormone peptides as imaging probes for primary and pulmonary metastatic melanoma detection. *J Nucl Med*. 2007; 48:73–80. [PubMed: 17204701]
6. Miao Y, Owen NK, Whitener D, Gallazzi F, Hoffman TJ, Quinn TP. In vivo evaluation of <sup>188</sup>Re labeled alpha-melanocyte stimulating hormone peptide analogs for melanoma therapy. *Int J Cancer*. 2002; 101:480–487. [PubMed: 12216078]
7. Miao Y, Owen NK, Hoffman TJ, Quinn TP. Therapeutic efficacy of a <sup>188</sup>Re labeled  $\alpha$ -melanocyte stimulating hormone peptide analog in murine and human melanoma-bearing mouse models. *J Nucl Med*. 2005; 46:121–129. [PubMed: 15632042]
8. Cheng Z, Chen J, Miao Y, Owen NK, Quinn TP, Jurisson SS. Modification of the structure of a metallopeptide: synthesis and biological evaluation of <sup>111</sup>In labeled DOTA conjugated rhenium cyclized alpha-MSH analogs. *J Med Chem*. 2002; 45:3048–3056. [PubMed: 12086490]
9. Miao Y, Hoffman TJ, Quinn TP. Tumor targeting properties of <sup>90</sup>Y and <sup>177</sup>Lu labeled alpha-melanocyte stimulating hormone peptide analogues in a murine melanoma model. *Nucl Med Biol*. 2005; 32:485–493. [PubMed: 15982579]
10. Miao Y, Hylarides M, Fisher DR, Shelton T, Moore H, Wester DW, Fritzberg AR, Winkelmann CT, Hoffman TJ, Quinn TP. Melanoma therapy via peptide-targeted  $\alpha$ -radiation. *Clin Cancer Res*. 2005; 11:5616–5621. [PubMed: 16061880]
11. Garmestani K, Milenic DE, Brady ED, Plascjak PS, Brechbiel MW. Purification of cyclotron-produced <sup>203</sup>Pb for labeling herceptin. *Nucl Med Biol*. 2005; 32:301–305. [PubMed: 15820766]
12. Milenic DE, Roselli M, Brechbiel MW, Pippin CG, McMurray TJ, Carrasquillo JA, Colcher D, Lambrecht R, Gansow OA, Schlom J. In vivo evaluation of a lead-labeled monoclonal antibody using the DOTA ligand. *Eur J Nucl Med*. 1998; 25:471–480. [PubMed: 9575242]
13. Chappell LL, Dadachova E, Milenic DE, Garmestani K, Wu C, Brechbiel MW. Synthesis, characterization, and evaluation of a novel bifunctional chelating agent for the lead isotopes <sup>203</sup>Pb and <sup>212</sup>Pb. *Nucl Med Biol*. 2000; 27:93–100. [PubMed: 10755652]
14. Chong HS, Milenic DE, Garmestani K, Brady ED, Arora H, Pfister C, Brechbiel MW. In vitro and in vivo evaluation of novel ligands for radioimmunotherapy. *Nucl Med Biol*. 2006; 33:459–467. [PubMed: 16720237]
15. Hui TE, Fisher DR, Kuhn JA, et al. A mouse model for calculating cross-organ beta doses from yttrium-90-labeled immunoconjugates. *Cancer*. 1994; 73(suppl):951–957. [PubMed: 8306284]
16. Beatty BG, Kuhn JA, Hui TE, Fisher DR, Williams LE, Beatty JD. Application of the cross-organ beta dose method for tissue dosimetry in tumor-bearing mice treated with a <sup>90</sup>Y-labeled immunoconjugate. *Cancer*. 1994; 73(suppl):958–965. [PubMed: 8306285]
17. Howell RW, Goddu SM, Narra VR, Fisher DR, Schenter RE, Rao DV. *Rad Res*. 1997; 147:342–348.

18. Carrasquillo JA, White JD, Paik CH, Raubitschek A, Le N, Rotman M, Brechbiel MW, Gansow OA, Top LE, Perentesis P, Reynolds JC, Nelson DL, Waldmann TA. Similarities and differences in  $^{111}\text{In}$ - and  $^{90}\text{Y}$ -labeled 1B4M-DTPA antiTac monoclonal antibody distribution. *J Nucl Med.* 1999; 40:268–276. [PubMed: 10025834]
19. Heppler A, Froidevaux S, Mäcke HR, Jermann E, Béhé M, Powell P, Hennig M. Radiometal-labeled macrocyclic chelator-derived somatostatin analogue with superb tumor-targeting properties and potential for receptor-mediated internal therapy. *Chem Eur J.* 1999; 5:1974–1981.
20. Liu S, Pietryka J, Ellars CE, Edwards DS. Comparison of yttrium and indium complexes of DOTA-BA and DOTA-MBA: model for  $^{90}\text{Y}$ - and  $^{111}\text{In}$ -labeled DOTA-biomolecule conjugates. *Bioconjugate Chem.* 2002; 13:902–913.

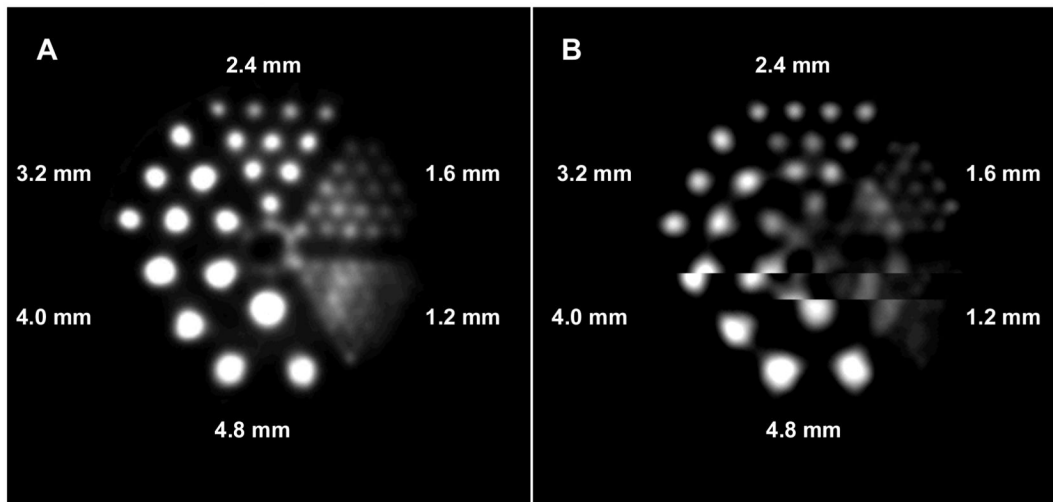


**Figure 1.**  
Phantom imaging of  $^{99m}\text{TcO}_4^-$  (A) and  $^{203}\text{PbCl}_2$  (B).

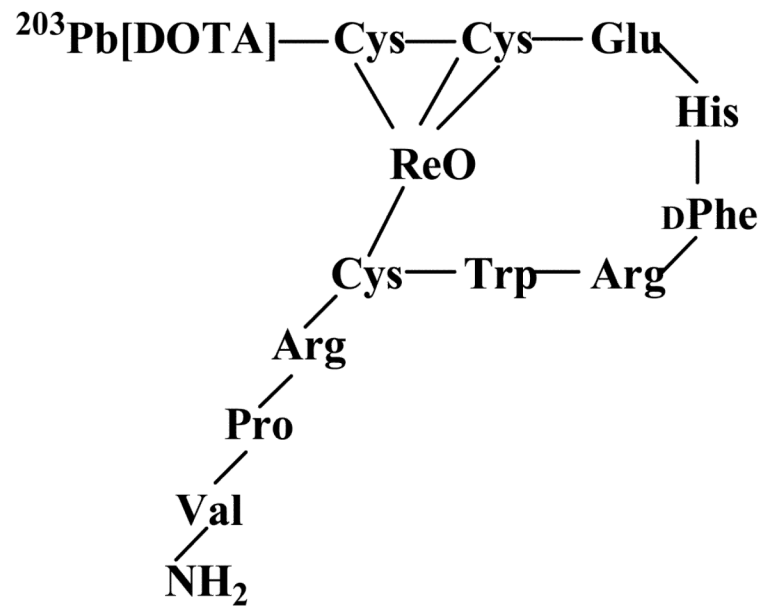


**Figure 2.**  
A schematic structure of the rhenium-cyclized peptide,  $^{203}\text{Pb}$ -DOTA-Re(Arg<sup>11</sup>)CCMSH.

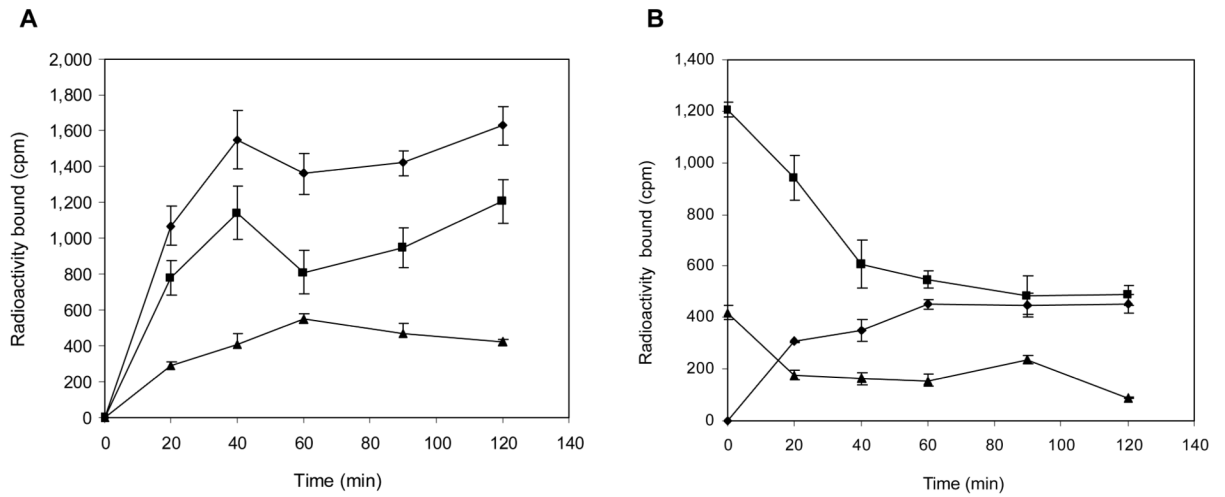


**Figure 3.** Cellular internalization (A) and efflux (B) of  $^{203}\text{Pb}$ -DOTA-Re(Arg<sup>11</sup>)CCMSH in B16/F1 murine melanoma cells at 25°C. Total bound radioactivity (◆), internalized activity (■), cell membrane activity (▲) and cell culture media activity (●) were presented as counts per minute (cpm).

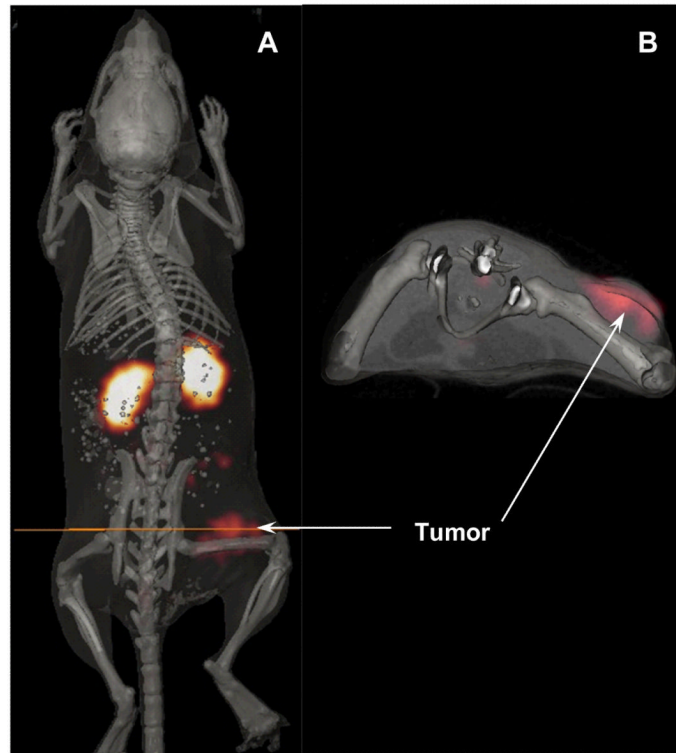


**Figure 4.** Whole-body (A) and transaxial (B) images with  $^{203}\text{Pb}$ -DOTA-Re(Arg<sup>11</sup>)CCMSH at 2 h post-injection in a B16/F1 murine melanoma-bearing C57 mouse.

Pharmacokinetics of  $^{203}\text{Pb}$ -DOTA-Re(Arg<sup>11</sup>)CCMSH in B16/F1 murine melanoma-bearing C57 mice. The data are presented as percent injected dose/gram or as percent injected dose (Mean $\pm$ SD, n = 5).

Table 1

Tissues	Percent injected dose/gram											
	5 min	30 min	1 h	2 h	4 h	24 h	48 h	2 h NDP				
Tumor	3.83 $\pm$ 0.87	8.79 $\pm$ 1.63	12.00 $\pm$ 3.20	11.87 $\pm$ 3.24	9.86 $\pm$ 1.86	4.35 $\pm$ 0.24	3.43 $\pm$ 1.12	0.88 $\pm$ 0.11				
Brain	0.35 $\pm$ 0.09	0.11 $\pm$ 0.04	0.04 $\pm$ 0.03	0.05 $\pm$ 0.03	0.02 $\pm$ 0.01	0.05 $\pm$ 0.04	0.06 $\pm$ 0.08	0.04 $\pm$ 0.02				
Blood	6.59 $\pm$ 0.57	2.10 $\pm$ 0.30	0.73 $\pm$ 0.09	0.39 $\pm$ 0.17	0.21 $\pm$ 0.09	0.28 $\pm$ 0.29	0.12 $\pm$ 0.03	0.64 $\pm$ 0.10				
Heart	3.07 $\pm$ 0.47	0.83 $\pm$ 0.07	0.33 $\pm$ 0.10	0.16 $\pm$ 0.05	0.06 $\pm$ 0.11	0.07 $\pm$ 0.07	0.07 $\pm$ 0.07	0.22 $\pm$ 0.04				
Lung	7.08 $\pm$ 1.38	2.24 $\pm$ 0.55	0.88 $\pm$ 0.05	0.41 $\pm$ 0.24	0.25 $\pm$ 0.12	0.22 $\pm$ 0.06	0.14 $\pm$ 0.10	0.57 $\pm$ 0.06				
Liver	2.49 $\pm$ 0.34	1.68 $\pm$ 0.22	1.25 $\pm$ 0.20	0.96 $\pm$ 0.26	0.62 $\pm$ 0.15	0.42 $\pm$ 0.07	0.36 $\pm$ 0.05	1.33 $\pm$ 0.39				
Spleen	2.54 $\pm$ 0.57	0.56 $\pm$ 0.29	0.43 $\pm$ 0.23	0.30 $\pm$ 0.09	0.26 $\pm$ 0.10	0.29 $\pm$ 0.15	0.15 $\pm$ 0.14	0.33 $\pm$ 0.08				
Stomach	1.42 $\pm$ 0.23	0.75 $\pm$ 0.15	0.31 $\pm$ 0.12	0.17 $\pm$ 0.13	0.06 $\pm$ 0.02	0.25 $\pm$ 0.26	0.14 $\pm$ 0.10	0.14 $\pm$ 0.05				
Kidneys	35.09 $\pm$ 6.42	10.31 $\pm$ 1.02	8.42 $\pm$ 0.36	7.78 $\pm$ 1.42	7.34 $\pm$ 0.31	3.69 $\pm$ 0.58	3.67 $\pm$ 0.50	9.0 $\pm$ 2.0				
Muscle	1.64 $\pm$ 0.63	0.44 $\pm$ 0.27	0.13 $\pm$ 0.03	0.05 $\pm$ 0.03	0.08 $\pm$ 0.05	0.06 $\pm$ 0.05	0.07 $\pm$ 0.03	0.05 $\pm$ 0.03				
Pancreas	1.76 $\pm$ 0.62	0.59 $\pm$ 0.35	0.40 $\pm$ 0.17	0.21 $\pm$ 0.07	0.11 $\pm$ 0.03	0.17 $\pm$ 0.11	0.09 $\pm$ 0.04	0.31 $\pm$ 0.11				
Bone	2.71 $\pm$ 0.16	1.89 $\pm$ 0.41	1.38 $\pm$ 0.16	1.01 $\pm$ 0.22	0.62 $\pm$ 0.18	1.11 $\pm$ 0.26	1.12 $\pm$ 0.26	1.05 $\pm$ 0.23				
Skin	3.58 $\pm$ 1.10	3.20 $\pm$ 0.21	1.14 $\pm$ 0.16	0.20 $\pm$ 0.07	0.28 $\pm$ 0.13	0.39 $\pm$ 0.31	0.37 $\pm$ 0.04	0.30 $\pm$ 0.08				
				Percent injected dose								
Intestines	4.60 $\pm$ 0.41	1.53 $\pm$ 0.12	0.95 $\pm$ 0.07	0.89 $\pm$ 0.06	0.55 $\pm$ 0.14	0.29 $\pm$ 0.05	0.27 $\pm$ 0.08	1.10 $\pm$ 0.18				
Urine	24.8 $\pm$ 5.0	74.73 $\pm$ 2.51	82.75 $\pm$ 3.98	89.02 $\pm$ 0.86	94.15 $\pm$ 0.31	93.34 $\pm$ 1.65	94.56 $\pm$ 1.13	91.34 $\pm$ 1.56				
				Uptake ratio of tumor/normal tissue								
Tumor/Blood	0.58	4.19	16.44	30.44	46.95	15.54	28.58	1.38				
Tumor/Kidneys	0.11	0.85	1.43	1.53	1.34	1.18	0.93	0.10				
Tumor/Liver	1.54	5.23	9.60	12.36	15.90	10.36	9.53	0.66				
Tumor/Muscle	2.34	19.98	92.31	237.40	123.25	54.38	49.00	17.60				

**Table 2**

Absorbed radiation doses per unit administered activity from  $^{203}\text{Pb}$ -DOTA-Re(Arg<sup>11</sup>)CCMSH in B16/F1 murine melanoma-bearing C57 mice.

Organ	$^{203}\text{Pb}$ -DOTA-Re(Arg <sup>11</sup> )CCMSH (Gy/37 MBq)
Tumor	4.32
Kidneys	4.35
Blood	0.56
Bone volume	0.50
Brain	0.06
Heart	0.08
Lung	0.16
Liver	0.35
Skin	0.10
Spleen	0.12
Stomach	0.06
Small intestine	0.11
Large intestine	0.26
Muscle	0.08
Pancreas	0.08
Remainder carcass	0.17